


Original Article

Bioenergetic influence on the historical development and decline of industrial fisheries

J. Guiet ^{1,2*}, E. D Galbraith^{1,3,4}, D. Bianchi¹, and W. W. L. Cheung⁵

¹Institut de Ciència i Tecnologia Ambientals (ICTA-UAB), Universitat Autònoma de Barcelona, 08193 Cerdanyola del Vallès, Barcelona, Spain

²Department of Atmospheric and Oceanic Sciences, University of California, Los Angeles, CA 90095, USA

³Institució Catalana de Recerca i Estudis Avançats (ICREA), Barcelona 08010, Spain

⁴Department of Earth and Planetary Science, McGill University, Montreal, QC, Canada

⁵Nippon Foundation-Nereus Program and Changing Ocean Research Unit, Institute for the Oceans and Fisheries, University of British Columbia, Vancouver, BC V6T1Z4, Canada

*Corresponding author: tel: +1 310 600 0662; e-mail: jerome.c.guiet@gmail.com.

Guiet, J., Galbraith, E. D., Bianchi, D., and Cheung, W. W. L. Bioenergetic influence on the historical development and decline of industrial fisheries. – ICES Journal of Marine Science, 77: 1854–1863.

Received 11 June 2019; revised 11 February 2020; accepted 13 February 2020; advance access publication 10 May 2020.

The global wild capture fishery expanded rapidly over the 20th century as fishing technology improved, peaking in the 1990s as most fisheries transitioned to fully- or over-exploited status. Historical records for individual large marine ecosystems (LMEs) tend to echo this same progression, but with local variations in the timing and abruptness of catch peaks. Here, we provide objective descriptions of these catch peaks, which generally progressed from high- to low-latitude LMEs, and attribute the temporal progression to a combination of economic and ecological factors. We show that the ecological factors can be remarkably strong by using a spatially resolved, observationally-constrained, coupled macroecological-economic model to which we impose an idealized, globally homogeneous increase in catchability. The globally-uniform technology creep produces a spatial progression of fishing from high-to-low latitudes that is similar to observations, primarily due to the impact of temperature on ecosystem metabolism. In colder LMEs, low respiration rates allow the build-up of larger pristine standing stocks, so that high-latitude fisheries are profitable earlier, at lower levels of fishing technology. We suggest that these bioenergetic characteristics contributed significantly to the historical progression of this human-ecological system.

Keywords: environmental driver, fisheries catch, large marine ecosystems, marine ecosystem model

Introduction

Historical reconstructions of wild fish catches show a steady increase in the global total until the 1990s, followed by a peak and plateau, or perhaps a slight decline (Pauly and Zeller, 2016; Watson, 2017). However, the smooth progression of globally summed catches hides dramatically different histories of fish stock exploitation at the local scale. For example, while catches in the Western Central Pacific and Indian oceans are still growing, catches in the Northern Atlantic, Mediterranean Sea and many other regions have been shrinking (Food and Agriculture Organization, 2014).

In general, the historical trajectories of most fisheries have been characterized by an early developing phase during which catches increased, followed by a peak when the fishery was fully exploited or over-exploited, followed by a decline in some duration (Grainger and Garcia, 1996). The decline could have been mitigated or eliminated where management efforts were able to prevent overfishing (Caddy and Cochrane, 2001; Hilborn and Ovando, 2014). As shown by Grainger and Garcia (1996), it appears that the sequential increase and decline in catches has shifted geographically over time, including a migration from higher- to lower-latitude regions.

© International Council for the Exploration of the Sea 2020.

This is an Open Access article distributed under the terms of the Creative Commons Attribution License (<http://creativecommons.org/licenses/by/4.0/>), which permits unrestricted reuse, distribution, and reproduction in any medium, provided the original work is properly cited.

Such regional differences in the historical trajectories of wild fish catch could have emerged from two types of factors: (i) spatial variation in human factors, including fish capture and processing technology, market forces, access to capital, or the imposition of regulations (Caddy and Cochrane, 2001; Watson *et al.*, 2013) and/or (ii) spatial variation in the environment-dependent characteristics of fish communities (Stock *et al.*, 2017; Van Denderen *et al.*, 2018). Unravelling the contributions of these different factors to the historical increase and decline in catches could provide an improved understanding of the underlying human-ecosystem dynamics.

Among other human factors, geographical differences in the accumulation of productive capital and the development of fishing technology clearly played a major role (Gelchu and Pauly, 2007). The level of capital and technologies for industrial fisheries to develop was first reached near North America after World War II, and subsequently near Europe and Japan. From there, they expanded to new ecosystems in other regions as fish demand increased and as stocks were depleted (Anticamara *et al.*, 2011; Bell *et al.*, 2017). This diffusion of fisheries from high-to-low latitudes (Swartz *et al.*, 2010) is likely to have contributed to the sequential progression of catches from high-to-low latitude. As high-latitude fisheries became depleted and as management measures were imposed to reduce effort, there was also a shift of fishing vessels to developing nations at lower latitudes (Alder and Sumaila, 2004). Thus, while management stimulated a stabilization or decline in catches at higher latitudes, it may indirectly have led to an increase in catches at lower latitudes (Watson *et al.*, 2014).

At the same time, environmental features undoubtedly contributed to variations between ecosystems by influencing the available fish biomass. For instance, it has been shown that fish production can be limited by the amount of energy available to coastal ecosystems from primary production (*PP*) (Jennings *et al.*, 2008; Chassot *et al.*, 2010), as well as water temperature (*T*), which influences the metabolic rates of ectotherms (Brown *et al.*, 2004; Clarke and Fraser, 2004). In multiple regions of the global ocean, temperature and *PP* differences have been shown to influence yields, along with factors related to the export of energy from pelagic food webs (Chassot *et al.*, 2010; Friedland *et al.*, 2012). In addition, there is growing appreciation for how the influence of climate change on *T* and *PP* will alter fish catches, with both single-stock and ecosystem-based models predicting significant declines under continued ocean warming (Carozza *et al.*, 2019; Free *et al.*, 2019; Lotze *et al.*, 2019). However, to our knowledge, the impact that spatial variations in these environmental conditions may have had on the historical progression of fisheries development has not previously been considered.

In this analysis, we provide objective descriptions of the catch reconstructions provided by the Sea Around Us Project (SAUP; Pauly and Zeller, 2015) at the scale of Large Marine Ecosystems (LMEs), 66 eco-regions of the World Ocean with distinct environmental characteristics. We first compare the resulting spatial progression of catch with an LME-level Human Development Index (HDI; United Nations Development Programme, 2016), with the expectation that a higher HDI would serve as a proxy for a greater degree of industrialization of fisheries. We also compare the observations with time-resolved numerical simulations using the global bioeconomic model BOATS (Carozza *et al.*, 2016, 2017). In the model, globally uniform technological progress in the fishery serves as the primary driver of long-term changes in fish catches (Galbraith *et al.*, 2017) so that spatial catch variations

emerge exclusively from environmental spatial variability. We then compare both the observed and modelled progressions with spatial patterns of temperature and *PP* and discuss mechanisms by which environmental drivers could have complemented socio-economic drivers in shaping the historical development and decline in industrial fisheries.

Material and methods

Observed catch in LMEs

LMEs account for 95% of the total wild fish catches while covering 22% of the global ocean surface (Stock *et al.*, 2017). These regions are differentiated based on environmental characteristics such as bathymetry, hydrography, *PP* and trophic relationships (Sherman and Duda, 1999), making them appropriate regional units to investigate the impact of the environment on the regional variability of historical time-series of fish catches. For each LME, the time-series of total catches over the period 1950–2013 has been reconstructed by SAUP (Pauly and Zeller, 2015) including industrial, artisanal, subsistence and recreational fishing as well as discarded catches. The high-seas regions outside LMEs are not included in the present study because of their low contribution to total wild catch.

There are 66 LMEs, all but one of which (the Central Arctic Ocean) are associated with historical total catch time-series. Following Friedland *et al.* (2012), we exclude from our study nine LMEs where data are incomplete or unreliable. These regions are the Antarctic, the Beaufort Sea, Chukchi Sea, East China Sea, East Siberian Sea, Hudson Bay, Kara Sea, Laptev Sea and Yellow Sea. The remaining 56 LMEs present various shapes of catch time-series (see Figure 1 and Supplementary Information S1). Most time-series show a widespread increase in catches explained by increasing effort and an improvement in technologies from 1950 onwards, but the detailed trajectories display diverse characteristics, with some regions passing through multiple large peaks of catches, like in the California Current (# 3), the Humboldt Current (# 13), or the Faroe Plateau (# 60). In these ecosystems, small pelagic fish are an abundant component of landings and sharp variations in these target species control fisheries yields (Pauly and Zeller, 2015). Other regions present an increase in catches up to a plateau, like in the East Bering Sea (# 1). These examples do not represent an exhaustive list of historic catch time-series trajectories [see Conti *et al.* (2012) for more details about the trends]. The most widespread feature of the time-series in LMEs is a monotonic increase in catches up to a maximum, like in the Bay of Bengal (# 34) or the Sulu-Celebes Sea (# 37), often followed by a monotonic decrease, like in the Sea of Japan (# 50) or the Central Pacific American Coast (# 11). A rebound in the catches may happen after this monotonic decrease, like in the South Brazil Shelf (# 15).

In this study, we focus on the catch time-series that present a clear peak in the total catch rate. We use objective criteria to extract these peaks from the 64 years of available data, following smoothing with a 6-year running average to filter out inter-annual variations. An LME is determined to include a clear peak when the 21 years of highest catches in the time-series occur almost sequentially within a 23-year period. With this criterion, we discard LMEs where there is not a clear dominant peak, as in the Faroe Plateau (# 60), the North Brazil Shelf (# 17), and the Aleutian Islands (# 65), and where the peak is embedded in a trend of rising catches, as in the California Current (# 3). We

retain 37 ecosystems out of the initial selection of 56 (Figure 1). Note that, with this method, a few of the identified peaks may be described as plateaux, without clear catch declines after the maxima. The conclusions of this study have little sensitivity to variations in the set of peaks selected (see [Supplementary Information S2](#)), or the details of the method for extracting the features of the peaks (Metrics for catch time-series and [Supplementary Information S3](#)).

Simulated catch with BOATS

The BOATS model simulates global wild capture fisheries on a 1° grid of the global ocean, as described in detail by [Carozza et al. \(2016, 2017\)](#). It consists of two modules, an ecological and an economic module.

The model represents the propagation of biomass $B(m)$ from lower- to upper-trophic levels assuming a direct link between individuals' size m and trophic level. This propagation corresponds to the growth of individuals and is constrained by PP and water temperature [see Environmental drivers (PP and T)]. Both variables directly influence the bioenergetics of individuals and thus indirectly control the biomass distribution. The ecological module provides the monthly distribution of biomass $B(m)$ (in tonnes of wet biomass, twB/m^2) of potential wild catch available to fishers between a minimum and maximum size $m \in [m_{\min}, m_{\max}]$.

The economic module simulates the dynamics of the effort E (in W/m^2) as a function of the profit, increasing in a grid cell when profit is positive and decreasing when profit is negative. Profit depends on the harvest that can be achieved from the biomass $B_{\text{tot}} \propto \int_{m_{\min}}^{m_{\max}} B(m) dm$ of wild catch available and is calculated as the balance between the costs $c = CE$ (C , cost per unit effort in $\$/\text{W}/\text{second}$) and revenues $r = pH$ (p , price per biomass unit in $\$/\text{twB}$) generated from the harvest $H \propto qB_{\text{tot}}E$

(in $\text{twB}/\text{m}^2/\text{second}$, where q is the biomass catchability per unit of effort in $\text{m}^2/\text{W}/\text{second}$) ([Gordon, 1954](#); [Schaefer, 1954](#)):

$$\frac{dE}{dt} = \kappa_e \frac{r - c}{E}, \quad (1)$$

where κ_e ($\text{W}^2/\text{m}^2/\$$) is a relaxation parameter representing fleet dynamics. The variation in effort per unit of profit ($r - c$) decreases with increasing fishing effort (as $1/E$). The inverse relationship between the rate of change and fishing effort reflects the fact that the portion of the total profit to be gained by individual fishers shrinks with total effort, weakening the motivation to move to the fishing grounds and thus slowing the adjustment of effort ([Gordon, 1954](#)).

We assume that, in most LMEs, there was minimal regulation until some time after peak LME catches, since the motivation to establish effective management was commonly provided by declining catches following overfishing ([Worm et al., 2009](#); [Hilborn and Ovando, 2014](#)). Thus, the historical development, peak and initial decline in catches at the LME level can be approximated by this open-access dynamics ([Galbraith et al., 2017](#)). The model simulates effort independently in each grid cell and, therefore, does not explicitly account for the spatial redistribution of effort from depleted regions to developing ones. Instead, spatio-temporal patterns emerge from differences in local dynamics ([Galbraith et al., 2017](#)).

Each BOATS simulation is a combination of a spin-up simulation that initializes the pristine (unfished) ocean, and a coupled biological-economic simulation reproducing the sequential development and decline in fishing in different regions ([Carozza et al., 2017](#)). An ensemble of five optimized sets of biological parameter values is used to span parameter uncertainty for the present study, as in [Galbraith et al. \(2017\)](#). In the economic module,

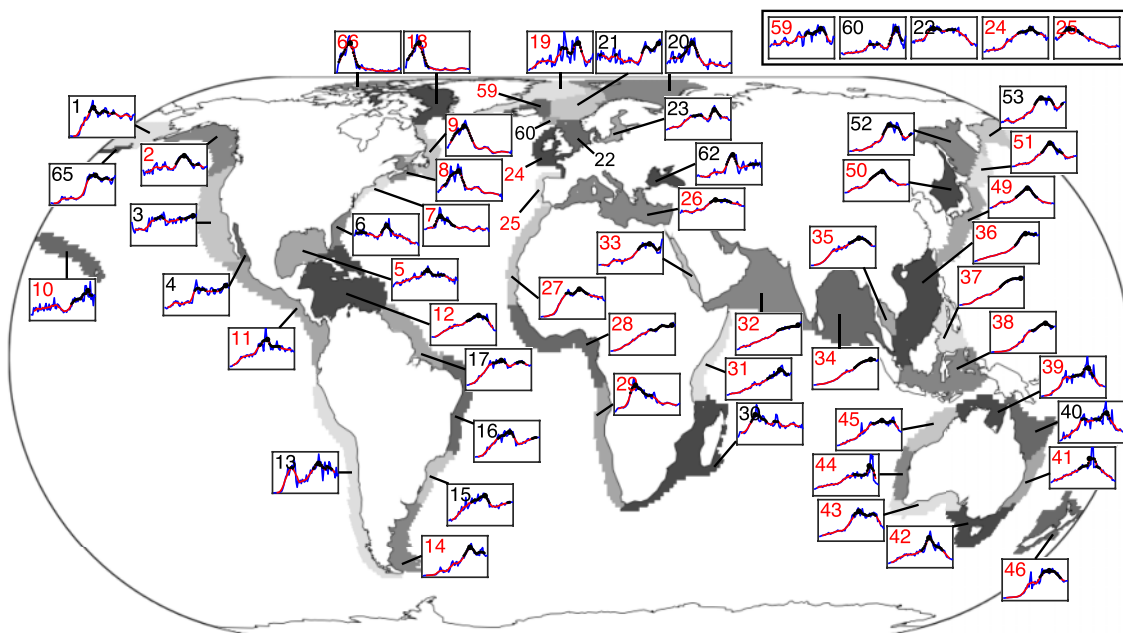


Figure 1. Total catch time-series per LME. Catch time-series from 1950 to 2013: blue lines, SAUP data; red lines, 6 years running average for the identification of the timing of catch peaks; black dots, 21 years of highest catches. Numbers refer to the list of LMEs detailed in [Supplementary Table S1](#), and numbers in red correspond to the 37 time-series where a peak is recognized. Note that five North Atlantic LMEs are plotted separately in the top right due to the lack of space on the map.

the catchability parameter q increases homogeneously at a rate r_q while cost and price (c and p) are held constant, since their historical role was likely secondary (Galbraith *et al.*, 2017).

We analysed the catch time-series by taking the mean of the five ensemble members and summing at the LME level. In addition, to explore the sensitivity of our results to different aspects of the model, we repeated the experiments using two additional rates of catchability increase r_p and excluding the effects of temperature and PP from specific components of the model (see Supplementary Information S4).

Metrics for catch time-series

Year of peak catches

The year of peak catches in each LME, $y_{\text{peak}}^{\text{LME}}$, is estimated for both observations and simulations. Observed catch time-series were smoothed with a 6-year running average. For each time-series, the year of peak catch is defined as the first year when 95% of the maximum catch is reached. This criterion is used to reduce the uncertainty in identifying the onset of long catch plateaux. We tested multiple methods of the selection of $y_{\text{peak}}^{\text{LME}}$ (see Supplementary Table S3a) and found relatively small sensitivity that would not influence our conclusions.

Time-series slopes

The slopes of pre-peak increase, $s_{\text{increase}}^{\text{LME}}$, and post-peak decrease, $s_{\text{decrease}}^{\text{LME}}$, are also determined on observed time-series smoothed with a 6-year running average and directly calculated from the model without applying any smoothing. The time-series are normalized by the maximum yield reached, allowing comparison of the relative speed of development and decline before and after the peaks. The increasing and decreasing time segments are identified by comparison to the maximal rates of change pre- and post-peak using the thresholds $[dH/dt > \max(dH/dt)/2.5]$ and $[dH/dt < \min(dH/dt)/2.5]$. The slopes over the identified segments are then calculated by linear regression. This method was empirically devised to provide robust diagnostics (see Supplementary Table S3b).

Investigated drivers

Environmental drivers (PP and T)

PP and temperature are the environmental drivers of fish production in BOATS. Following Carozza *et al.* (2016), we use monthly climatologies of temperature from the World Ocean Atlas 2005 (Locarnini *et al.*, 2006). In each $1^\circ \times 1^\circ$ grid cell, we use average temperature over the upper 75 m. For PP , we take the average of three satellite-based net PP estimates (Behrenfeld and Falkowski, 1997; Carr *et al.*, 2006; Marra *et al.*, 2007) to capture some of the variability that exists in different models. Similar to temperature, we use monthly climatologies on a $1^\circ \times 1^\circ$ grid. For comparison to observed peaks, we take the annual mean of these drivers over LMEs.

Human Development Index

The HDI attempts to capture the average achievement in terms of life expectancy, level of knowledge, and standard of living and is available at the country level (United Nations Development Programme, 2016). Here, it is used as a proxy for the level of technological development of the fisheries of distinct nationalities involved in a given LME. Weighted according to the catches of each nation operating in the LME, we take it as a proxy of the

technology level of fleets fishing in the LME. We reconstruct the HDI time-series for each LME, $\text{HDI}^{\text{LME}}(y)$, from the HDI of each country $\text{HDI}_{\text{country}}$, and the historical catches per LME of each country $H^{\text{LME}}(\text{country}, y)$ between the year $y = 1950$ and 2013, as provided by SAUP (Pauly and Zeller, 2015):

$$\text{HDI}^{\text{LME}}(y) = \frac{\sum_{\text{country}} \text{HDI}_{\text{country}} H^{\text{LME}}(\text{country}, y)}{\sum_{\text{country}} H^{\text{LME}}(\text{country}, y)}. \quad (2)$$

The resulting time-series indicates the average level of development for each LME over time, due to changes in the relative contribution of different national fleets to the total catches. We compare the mean HDI per LME between 1950 and 2013, HDI^{LME} , as well as variation $\Delta\text{HDI}^{\text{LME}} = \text{HDI}^{\text{LME}}(2013) - \text{HDI}^{\text{LME}}(1950)$, with the $y_{\text{peak}}^{\text{LME}}$.

Results

Observed history of peak catches

Among the 56 historical catch time-series analysed (Figure 1 and Supplementary Information S1), our objective criteria identify 37 catch peaks (see Supplementary Table S2 for results on different sets of LMEs). The year of peak catches for each, $y_{\text{peak}}^{\text{LME}}$, shows a discernible spatial progression between different parts of the global ocean (see Figure 2a). The peaks occurred first in the 1960s in the Northwest Atlantic. Tropical LMEs are generally the last to reach their peaks with some still developing in 2013, such as the Sulu-Celebes Sea (# 37).

Comparison with HDI

Geographical variations in social and economic characteristics of fishing nations have been widely documented (Gelchu and Pauly, 2007; Anticamara *et al.*, 2011; Bell *et al.*, 2017). We therefore carried out a comparison of our catch peak years and the corresponding catch-weighted HDI in each LME by calculating their pairwise coefficients of determination.

When we compare the year of peak catch $y_{\text{peak}}^{\text{LME}}$ to the historical level of societal development of LMEs encapsulated in HDI^{LME} , we found a significant negative correlation ($R^2 = 0.13$ and $p < 0.05$, see Figure 3 and summary Table 1). This is consistent with the expectation that LMEs exploited at higher HDI would have reached peak catches earlier.

In addition, changes in HDI^{LME} between 1950 and 2013 can be constructed from changes in the composition of nations fishing within the LME. We use the $\Delta\text{HDI}^{\text{LME}} = \text{HDI}^{\text{LME}}(2013) - \text{HDI}^{\text{LME}}(1950)$ to test for the invasion of long-distance fleets in low-latitude waters. Relatively few LMEs appear to have had large invasions of long-distance fleets by this measure (see size of markers Figure 3 and Supplementary Information S5), among them the Guinea Current (# 28), the Somalia Current (# 31), and the Red Sea (# 33). These invasions should have had a slight influence on the correlation between $y_{\text{peak}}^{\text{LME}}$ and HDI^{LME} (Table 1).

Simulated history of peak catches

The BOATS model simulates the temporal evolution of fisheries as driven by a globally homogeneous increase in catchability, which represents the net outcome of all aspects of technological progress on the ability to catch the available fish with a given effort. Given the global uniformity of catchability change, the differences in simulated peak years among LMEs depend only on

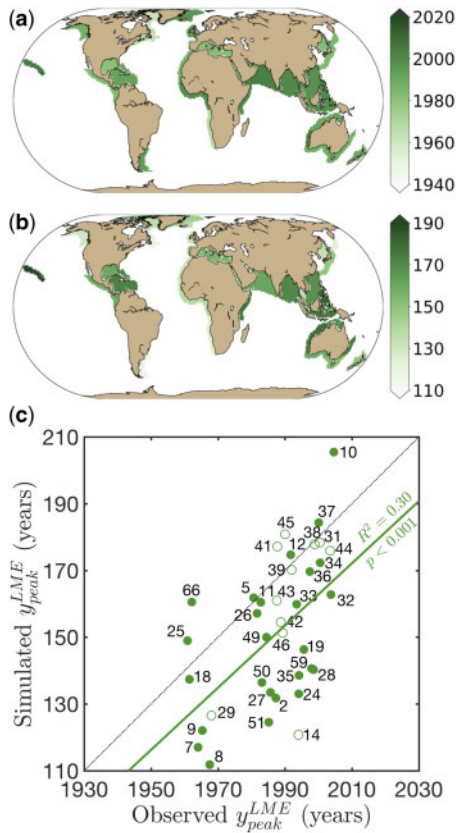


Figure 2. Observed and simulated years of maximum catch. Spatial progression of the year of peak catches y_{peak}^{LME} in the 37 LMEs selected: (a) observations, (b) simulations, and (c) simulated vs. observed year of peak catches ($y = 9.32 \times 10^{-1}x + 1700$, $R^2 = 0.30$, $p < 10^{-3}$). The solid line is a linear fit through the observed and simulated timings of peaks, and the dotted line is the 1:1 slope. The empty circles indicate LMEs in the Southern Hemisphere, and the filled circles indicate LMEs in the Northern Hemisphere.

environmental differences between grid cells. Perhaps surprisingly, despite globally homogeneous technological and economic conditions, the simulations show a global spatial progression of fishing that is broadly similar to the observations, with peaks occurring first at high latitudes, and subsequently at low latitudes (see Figure 2b). The simulated LME peak years are significantly correlated with observations where a peak of catches is identified ($R^2 = 0.30$, $p < 10^{-3}$, Figure 2c and Table 1), despite the large number of confounding processes. This result holds for different sets of LMEs (Supplementary Table S2), as well as when we include all 56 LMEs, although it is weaker in this case ($R^2 = 0.15$, $p < 0.01$, see Supplementary Figure S6a). The model suggests a slower sequential development of fishing than observed, as revealed by the larger spread of the years of peak catch in the simulations (Figure 2c). This feature is related to the rate of catchability increase, here $r_q = 5\%$. A higher rate would compress the interval between the first and the last occurrences of LMEs maximum harvests, while a lower rate would have the opposite effect (see Supplementary Information S4).

It might be expected that fisheries management has had an influence on the year of maximum catches in some ecosystems, an

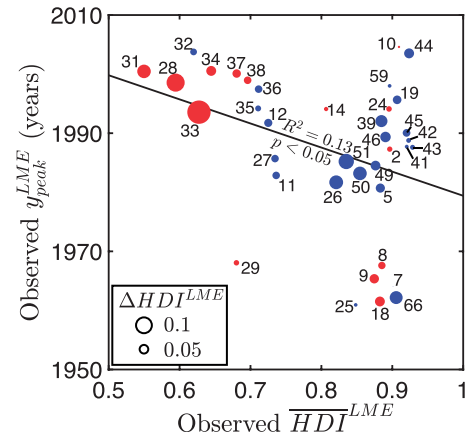


Figure 3. Socio-economic influence on the observed and simulated catch peaks. Year of maximum catches y_{peak}^{LME} as a function of mean HDI^{LME} in the 37 selected LMEs ($y = -40.8x + 2020$, $R^2 = 0.13$, $p < 0.05$). The diameter of the markers is proportional to $\Delta HDI^{LME} = HDI^{LME}(2013) - HDI^{LME}(1950)$, which expresses changes in the composition of nations fishing within the LME, red positive, blue negative.

Table 1. Summary of linear regressions: slope, R^2 , and p -value.

Variable 1	Variable 2	Slope	R^2	p -Value
Human Development Index (HDI^{LME})	Obs. y_{peak}^{LME}	-40.8	0.13	<0.05
	Obs. y_{peak}^{LME}	Sim. y_{peak}^{LME}	9.32×10^{-1}	0.30
Temperature (T)	Sim. y_{peak}^{LME}	1.53	0.44	< 10^{-5}
	Obs. y_{peak}^{LME}	7.73×10^{-1}	0.33	< 10^{-3}
	Sim. $s_{increase}^{LME}$	-1.62×10^{-4}	0.12	<0.05
	Obs. $s_{increase}^{LME}$	-6.89×10^{-4}	0.09	>0.05
	Sim. $s_{increase}^{LME}$	1.68×10^{-4}	0.29	< 10^{-3}
	Obs. $s_{increase}^{LME}$	1.87×10^{-3}	0.33	<0.01
Primary production (PP)	Sim. y_{peak}^{LME}	-9.56×10^{-2}	0.09	>0.05
	Obs. y_{peak}^{LME}	1.46×10^{-2}	0.01	>0.05

effect that is absent in the model. In an attempt to detect this, we removed particularly well-managed LMEs such as the Australian LMEs (# 39 and 41–45; Flood et al., 2014). However, this did not increase the coefficient of determination between simulations and observations ($R^2 = 0.29$, $p < 0.01$, see Supplementary Figure S6b).

An additional consideration is that some LMEs contain small regions with very high or low PP as inferred from satellite, a fact that may challenge the model’s ability to correctly resolve biomass production. For example, in some LMEs, the PP is concentrated in the vicinity of the mouth of major rivers, such as in the Patagonian Shelf (# 14), the Guinea current (# 28), or the Gulf of Thailand (# 35). Because the model does not resolve the movement of fish or their prey, it may overestimate fish density in these localized highly productive regions, leading to an earlier peak in catches compared with observations. Indeed, when we remove the most heterogeneous LMEs from the 37 selected, the coefficient of determination increases substantially

($R^2 = 0.43$, $p < 10^{-4}$, see [Supplementary Figures S6c and S7](#) summarizing the heterogeneity of T and PP across each LME).

We note that the inclusion of unreported catch estimates in the SAUP reconstructions influences the results to some degree. When only reported catches are considered to determine the year of peak catch, the coefficient of determination between simulations and observations is weaker ($R^2 = 0.15$, $p < 0.05$, see [Supplementary Figure S6d](#)). However, the removal of unreported catches does not strongly alter the sequence of $y_{\text{peak}}^{\text{LME}}$ for most LMEs and the low coefficient of determination is largely attributable to the Insular Pacific-Hawaiian LME (# 10). Thus, our results generally apply to reported catch time-series as well.

Comparison with environmental drivers

Given that the model broadly reproduces the observed trends of $y_{\text{peak}}^{\text{LME}}$, we next consider how the bioenergetic mechanisms at play in the model might have contributed to the historical timing of catch peaks, while bearing in mind that socio-economic factors are certain to have also contributed in reality.

As with the HDI above, relationships between the catch peaks and the environmental drivers can be roughly assessed by calculating their pairwise coefficients of determination. In the model, $y_{\text{peak}}^{\text{LME}}$ is strongly correlated with T in the 37 LMEs with unambiguous catch peaks ($R^2 = 0.44$, $p < 10^{-5}$, see [Figure 4a](#), in black) but is not significantly correlated with PP (see [Table 1](#) and [Supplementary Figure S8](#)). A very similar pattern emerges in the observations, where no correlation is found between $y_{\text{peak}}^{\text{LME}}$ and PP , but a stronger coefficient of determination is found with T ($R^2 = 0.33$, $p < 10^{-3}$ see [Figure 4a](#), in blue, or [Supplementary Information S9](#) for the same figure with LME numbers, and [Table 1](#)). The correlation between $y_{\text{peak}}^{\text{LME}}$ and T is largely independent of the set of LMEs selected, with the correlations remaining significant when we consider alternate sets of LMEs, or even all 56 LMEs with reliable catch time-series (see [Supplementary Information S2 and S10](#)).

Surprisingly, the correlation between $\overline{\text{HDI}}^{\text{LME}}$ and $y_{\text{peak}}^{\text{LME}}$ is not as strong as the correlation between $y_{\text{peak}}^{\text{LME}}$ and LME temperature (see [Table 1](#)). In addition, while $\overline{\text{HDI}}^{\text{LME}}$ correlates with ecosystem temperature, when we carried out a multiple linear regression of $y_{\text{peak}}^{\text{LME}}$ with both temperature and $\overline{\text{HDI}}^{\text{LME}}$, there was no improvement over the regression using only temperature (see adjusted R^2 in [Supplementary Table S5a](#)) and only temperature was a significant predictor ([Supplementary Table S5b](#)). Thus, HDI does not appear to be a better predictor of $y_{\text{peak}}^{\text{LME}}$ than ecosystem temperature.

We also tested whether or not the slopes associated with catch peaks are correlated with the environmental drivers. The modelled $s_{\text{increase}}^{\text{LME}}$ is only weakly correlated with T , and the observed slope is not significantly correlated (see [Table 1](#), [Figure 4b](#), and [Supplementary Information S2](#) for sensitivity tests), suggesting negligible influence on $s_{\text{increase}}^{\text{LME}}$. In contrast, the rate of relative decrease $s_{\text{decrease}}^{\text{LME}}$ is significantly correlated with T , both in the model ($R^2 = 0.29$, $p < 10^{-3}$, see [Figure 4c](#), in black) and in observations ($R^2 = 0.33$, $p < 0.01$, see [Figure 4c](#), in blue, [Supplementary Information S9](#) for the figure with LME numbers, [Table 1](#), and [Supplementary Information S2](#) for sensitivity tests). Note that, because of the irregularity of observed catch time-series, the determination of the slopes remains more uncertain than the determination of the peak years (see [Supplementary Information S3](#)).

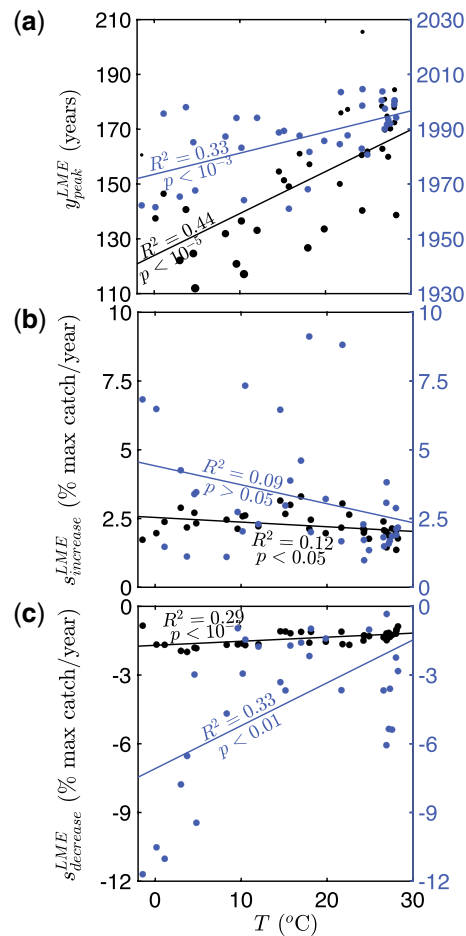


Figure 4. Influence of temperature on the features of observed and simulated catch peaks. Features in selected LMEs as a function of the mean annual water temperature T : (a) year of peak $y_{\text{peak}}^{\text{LME}}$, simulations in black ($y = 1.53x + 124$, $R^2 = 0.44$, $p < 10^{-5}$) and observations in blue ($y = 7.73 \times 10^{-1}x + 1974$, $R^2 = 0.33$, $p < 10^{-3}$); (b) slopes $s_{\text{increase}}^{\text{LME}}$, simulations in black ($y = -1.62 \times 10^{-4}x + 2.54 \times 10^{-2}$, $R^2 = 0.12$, $p < 0.05$) and observations in blue ($y = -6.89 \times 10^{-4}x + 4.42 \times 10^{-2}$, $R^2 = 0.09$, $p > 0.05$); (c) slopes $s_{\text{decrease}}^{\text{LME}}$, simulations in black ($y = 1.68 \times 10^{-4}x - 1.71 \times 10^{-2}$, $R^2 = 0.29$, $p < 10^{-3}$) and observations in blue ($y = 1.87 \times 10^{-3}x - 7.08 \times 10^{-2}$, $R^2 = 0.33$, $p < 0.01$). In (a), the size of the black markers reflects the standing biomass at the beginning of exploitation. The solid lines are linear fits through the observed and simulated features of the peaks.

Although these correlations do not provide direct evidence of a causal relationship, they are consistent with metabolism-based expectations that water temperature should exert a direct bioenergetic control on fish abundance and production rates, thereby interacting with fishing. A strong role for temperature in the model is further confirmed by an alternate simulation where all effects of temperature are removed (see [Supplementary Information S4](#)). In this case, the correlation between modelled and observed $y_{\text{peak}}^{\text{LME}}$ disappears. The lack of a significant role for PP does not reflect a lack of importance, since it plays a major role in limiting fish production in the model [Carozza et al. \(2016\)](#); however, PP does not emerge as a useful predictor of the timing of harvest peaks.

Water temperature can alter many vital aspects of marine ectothermic animals, including feeding rates ([Rall et al., 2012](#)),

growth, mortality and reproduction (Brown *et al.*, 2004; Clarke and Fraser, 2004), and respiration (Clarke and Johnston, 1999) with consequent impacts on the dissipation rate of biomass energy (Guiet *et al.*, 2016). These direct temperature effects are represented in the model by Arrhenius dependences (Carozza *et al.*, 2016), which predict averaged rate increases of 60–110% for every 10°C temperature increase, for different parameter ensembles, and 87% for the ensemble mean. They affect growth, reproduction, and mortality. BOATS does not explicitly include the temperature-dependent respiration associated with activity and reproduction, but these processes are included implicitly in the losses due to temperature-dependent mortality (Carozza *et al.*, 2019). Water temperatures also influence the modelled trophic transfer of energy because cold waters tend to be characterized by larger phytoplankton cells, which are in turn consumed by larger predators, shortening food webs (Stock and Dunne, 2010). In the model, this size of phytoplankton is computed from *PP* and temperature with an empirical formulation (Dunne *et al.*, 2005). These temperature dependencies alter both the initial standing biomass and the replacement rate of fished biomass by recruitment and growth. Each of these two factors impacts the interaction with fishing effort in a different way, by modifying the year of peak catches and the rate of decline, respectively, as we discuss next.

Temperature influence on initial biomass

In the pristine state (i.e. prior to fishing), simulated cold LMEs support a higher biomass density than warm LMEs (see Figure 5a, $B_{\text{tot}}^{\text{cold}} > B_{\text{tot}}^{\text{warm}}$ and Figure 4a, size of black markers). In the model, T influences the pristine biomass through its effects on mortality, representative size of phytoplankton and growth rates. Among the effects, the temperature impact on mortality is the most important. Phytoplankton size and growth rates have a secondary impact (see sensitivity experiments in the Supplementary Information S4). The general model prediction agrees with theoretical (Ursin, 1984) and other modelling studies (Jennings *et al.*, 2008).

All else being equal, high biomass densities would be expected to yield a greater catch for a given amount of effort and are therefore more likely to be profitable with relatively primitive fishing technologies. Thus, cold locations with larger pristine biomass densities would be expected to have been exploited first. This can be understood by considering a critical level of biomass B_{crit} , defined as the minimum biomass at which exploitation is profitable. Under the simple assumption of economic open access, this occurs when the revenue $r = pH = pqB_{\text{crit}}E$ (where p is the ex-vessel price, H is the wild fish harvest, q is the catchability, and E is the effort) is equal to the associated costs of fishing, $c = CE$ (C = cost per unit effort; see model description in Material and Methods). This implies that $B_{\text{crit}} = C/pq$, so that given fixed C and p , the B_{crit} is determined by q alone (Carozza *et al.*, 2017), and decreases with increasing q . In our increasing-technology experiments, fishing begins at any given location when q rises to the point at which B_{crit} is equal to the local standing biomass. These mechanisms bear some resemblance to “basin models”, in which a geographically resolved habitat suitability controls production, and fishing activity is proportional to the local biomass (MacCall, 1990).

Figure 5a illustrates this mechanism, comparing two regions with different temperatures, the warmer Caribbean Sea (# 12)

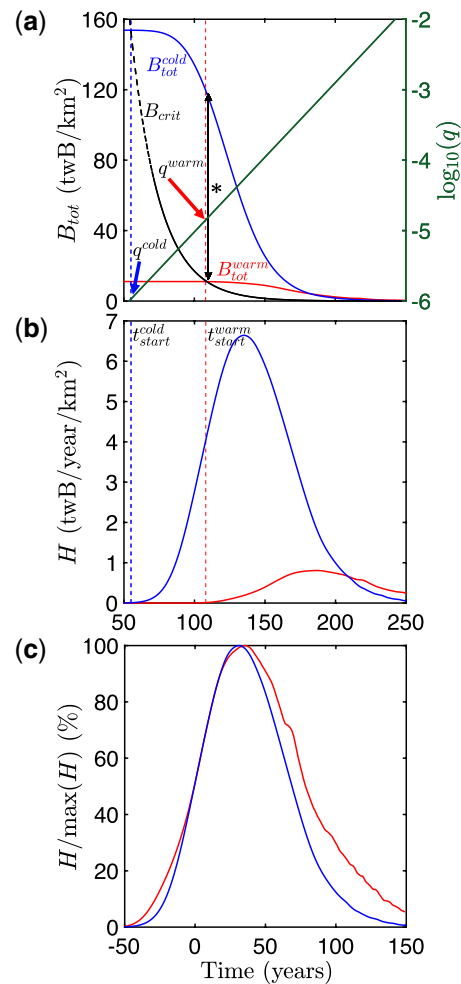


Figure 5. Schematic representation of the history of simulated catch time-series in cold and warm ecosystems. Comparison of simulated biomass decrease (a), total catch peak (b) and catch peaks normalized by the maximum catches and centred around the mid-catch peak (c): in a colder (blue) ecosystem, the Benguela Current (# 29), $\bar{T} = 18^\circ\text{C}$; in a warmer (red) ecosystem, the Caribbean Sea (# 12), $\bar{T} = 27^\circ\text{C}$. In green, the logarithm of the catchability increases over years. While catchability increases, ecosystems with a lower standing biomass $B_{\text{tot}}^{\text{cold/warm}}$ begin to be exploited when the biomass is equal to the critical biomass level allowing the onset of fishing $B_{\text{crit}} = C/pq$, black dashed line. The vertical dashed lines indicate the beginning of exploitation. In (a), the black vertical arrow (*) indicates the degree to which the cold water biomass B_{cold} is out of equilibrium with the evolving q at the point where fishing begins on B_{warm} .

and the colder Benguela Current (# 29). Fisheries develop first in cold regions with a higher standing biomass, when $B_{\text{crit}} = B_{\text{cold}}$ (at $q = q^{\text{cold}}$). Subsequently, when the catchability has increased sufficiently such that $B_{\text{crit}} = B_{\text{warm}}$ (at $q = q^{\text{warm}}$), fishing begins in the warm region. Note that the simulated extraction of biomass illustrated in Figure 5a proceeds slowly enough that the biomass B_{cold} remains higher than B_{crit} throughout. Because of this non-equilibrium behaviour, the B_{cold} at the time that q reaches q^{warm} remains higher than the corresponding B_{warm} . Moreover, for a continuous increase in catchability q , B_{crit} inexorably decreases, as smaller and smaller biomasses become

profitable to fisheries, driving biomass and ultimately catches towards zero. Thus, by influencing the pristine biomass of ecosystems, the temperature is expected to influence the technology level under which fishing first becomes profitable.

Temperature influence on biomass replacement rate

In the model, higher water temperatures lead to faster growth and reproduction rates. As a result, despite large pristine biomasses, cold LMEs have slower biomass production per unit of biomass compared with warm LMEs with similar primary productivity. Thus, warm ecosystems have faster biomass turnover, replacing their standing biomass more quickly. In the meantime, the model predicts smaller phytoplankton in warmer waters, so that the energy available for recruits and growth at a given fish size is reduced in warmer ecosystems. The mortality rate also increases in warmer waters. When fishing begins, these effects influence the shape of peaks in the catch time-series.

In [Figure 5b](#), the simulated peak of fishing is more gradual at a warm site than at a cold site. When normalized by the maximum total catches (see [Figure 5c](#)), the increasing slopes at the two sites are similar, but the peak is longer and the decline is more gradual at the warm site. This dynamic is consistent with the correlation between water temperature and $s_{\text{decrease}}^{\text{LME}}$ (cf [Figure 4c](#)), despite the lack of correlation with the rate of increase (cf [Table 1](#) and [Figure 4b](#)). We suggest that increasing catchability dominates the catch increase, therefore supporting similar trends of rising catch, while temperature-dependent biomass replacement rates influence the rate of catch decrease. Sensitivity tests with the model confirm the role of temperature on the biomass turnover in warm waters, arising from faster reproduction and growth of ectotherms, convolved with variations in the phytoplankton representative size that limits recruitment (see [Supplementary Information S4](#)).

Discussion

The observed temporal progression of catches across the global ocean is largely consistent with the expectation from spatial variations in economic development, but also with the expected impacts of spatial variations in water temperature. Specifically, the observed year of peak catch occurred earlier in ecosystems with higher HDI and in colder water, while the rate of post-peak catch decline was more rapid in colder water. *PP* alone was not a good predictor of the year of historical catch peaks. While differences in the accumulation of capital and technological development undoubtedly explain a good part of these historical progressions, our results suggest that the impact of water temperature on ecosystem metabolism played a complementary role. Most importantly, greater pristine standing biomass density should have allowed an earlier development of profit-driven industrial fisheries in cold waters, while fishing technology was less advanced. More rapid turnover of biomass and recruitment in warm waters is likely to have played a secondary role, contributing to slower post-peak declines in catches at low latitudes.

Uncertainty in observed LME-level correlations

The analysis above was carried out at the coarse scale of LMEs and annually averaged observations, potentially masking finer-scale spatio-temporal variations that could impact the strength of our correlations. However, since many fish species are migratory, an analysis at finer spatial scales would raise other issues, such as

potential mismatches between spawning grounds, feeding grounds, and the regions where fish are caught. A complementary analysis is provided in [Supplementary Information S11](#) by looking at the catch time-series according to exclusive economic zones (EEZs). This analysis shows weaker correlations with temperature than at the LME scale, which may reflect the fact that some EEZs span multiple ecosystems, blurring environmental distinctions, while in other cases, a single ecosystem is partitioned between multiple EEZs, potentially separating fishing grounds from regions of biomass production. The weaker correlations may also reflect an accentuation of country-specific social and economic factors that cloud the environmental influence.

Our analysis also relies on reconstructions of catch time-series from SAUP with their own inherent uncertainties. We assessed the degree to which the correlation between catch peak years and LME temperature is robust to the set of LMEs selected by varying the parameters of our method to identify large catch peaks in time-series (see [Supplementary Information S2](#)) and by isolating distinct sets according to the characteristics of the environment and the management (see [Supplementary Information S6](#)). The correlation remains significant when our method is applied to the catch time-series before reconstruction ([Supplementary Information S6](#)) or even when applied to the 56 LMEs ([Supplementary Information S10](#)). Thus, the covariation of the year of maximum catch at LME with ecosystem temperature appears to be robust.

Individual stocks vs. LME-level changes

In the analysis above, we only consider aggregated time-series of the total catch. The aggregation conceals the fact that different species and stocks within a given ecosystem can vary in terms of their economic features, catchability, and vulnerability to exploitation ([Cheung et al., 2007](#)). The vulnerability depends on stock-specific factors including the maximum length, the age at first maturity, the fecundity, and the growth rate. Conceivably, these different features of individual stocks could influence the development and decline in fisheries preferentially targeting these stocks, influencing the sequential succession of stock exploitations and thereby influencing the shape and timing of the LME catch peak (see [Supplementary Information S12](#)).

However, an analysis of SAUP catch records carried out at the species level does not indicate systematic features that would bias the LME-level aggregation ([Supplementary Information S12](#)). The timing of peak catch years for individual stocks was not systematically related to the year of peak catch, and post-peak declines in individual stocks were similar to those of the LMEs in which they are found. We therefore conclude that species-level effects do not play a major role in determining the LME-level peak year and post-peak decline.

Mechanisms beyond bioenergetics

Any model presents, by necessity, a simplified view of a complex global ecosystem. In the model used here, the temperature effect on growth, recruitment, and mortality rates places the dominant control on standing biomasses, and thereby the development and decline of fishing, but temperature also covaries with other environmental factors that can influence standing biomasses that are not explicitly included in the model. For example, extensive continental shelves allow high fractions of benthic production that can accumulate high biomass and are also easily exploited ([Van](#)

Denderen *et al.*, 2018). In addition, the higher diversity of exploitable fish species in warm, low-latitude ecosystems could cause harvest peaks to be extended as fishers shift from one stock to the next, decreasing the slope of post-peak declines (Maureaud *et al.*, 2019). Finally, the simple features of our economic model place technological development as the dominant drivers and ignore other such as changes in profitability that may have occurred when fisheries change targeted species as they move equatorward, or changes in cost as steaming distance from port increases. Accounting for these additional effects would add further nuance to the historical progression of global fisheries.

Concluding remarks

While spatially variable socio-economic drivers certainly influenced the historical progression of industrial fishing from high latitudes to the tropics, our results indicate the likelihood that ecosystem temperature also played a role through its influence on the biological component of these coupled ecological-economic systems. The observed correlations between the year of peak catch and HDI are not stronger than those with temperature, and our bioeconomic model produced a progression similar to the observations when forced only with a globally homogeneous progression of technological development. Together, these findings emphasize the role that ecosystem temperature could have played in shaping the historical development of fisheries over the past 70 years.

The recognition that temperature, via its influence on ecosystem-level metabolism, could have contributed to the historical progression of fisheries provides a new perspective on these complex human-ecological systems. Importantly, it is consistent with the expected changes in fisheries productivity under climate change, with warmer ecosystems supporting less fish biomass and lower maximum sustainable yields (Cheung *et al.*, 2010; Carozza *et al.*, 2019; Lotze *et al.*, 2019; Free *et al.*, 2019). In addition, the fact that water temperature has opposing influences on biomass accumulation vs. biomass replacement suggests that the outcome of future warming on fish catches will vary with fishing pressure. These findings provide support for a greater emphasis on temperature-dependent ecosystem bioenergetics, which considers the long-term outlook for fisheries.

Supplementary data

Supplementary material is available at the *ICESJMS* online version of the manuscript.

Funding

This study has received funding from the European Research Council (ERC) under the European Union's Horizon 2020 research and innovation programme (682602) and support from the Spanish Ministry of Economy and Competitiveness, through the Maria de Maeztu Programme for Centres/Units of Excellence in RD (MDM-2015-0552). JG and DB acknowledge support from NASA grant TunaScape (award 80NSSC17K0290) and California Department of Resources-Ocean Protection Council (C0100400).

References

Alder, J., and Sumaila, U. R. 2004. Western Africa: a fish basket of Europe past and present. *The Journal of Environment & Development*, 13: 156–178.

- Anticamara, J., Watson, R., Gelchu, A., and Pauly, D. 2011. Global fishing effort (1950–2010): trends, gaps, and implications. *Fisheries Research*, 107: 131–136.
- Behrenfeld, M. J., and Falkowski, P. G. 1997. Photosynthetic rates derived from satellite-based chlorophyll concentration. *Limnology and Oceanography*, 42: 1–20.
- Bell, J. D., Watson, R. A., and Ye, Y. 2017. Global fishing capacity and fishing effort from 1950 to 2012. *Fish and Fisheries*, 18: 489–505.
- Brown, J. H., Gillooly, J. F., Allen, A. P., Savage, V. M., and West, G. B. 2004. Toward a metabolic theory of ecology. *Ecology*, 85: 1771–1789.
- Caddy, J., and Cochrane, K. 2001. A review of fisheries management past and present and some future perspectives for the third millennium. *Ocean & Coastal Management*, 44: 653–682.
- Carozza, D. A., Bianchi, D., and Galbraith, E. D. 2016. The ecological module of BOATS-1.0: a bioenergetically constrained model of marine upper trophic levels suitable for studies of fisheries and ocean biogeochemistry. *Geoscientific Model Development*, 9: 1545–1565.
- Carozza, D. A., Bianchi, D., and Galbraith, E. D. 2017. Formulation, general features and global calibration of a bioenergetically-constrained fishery model. *PLoS One*, 12: 1–28.
- Carozza, D. A., Bianchi, D., and Galbraith, E. D. 2019. Metabolic impacts of climate change on marine ecosystems: implications for fish communities and fisheries. *Global Ecology and Biogeography*, 28: 158–169.
- Carr, M.-E., Friedrichs, M. A., Schmeltz, M., Aita, M. N., Antoine, D., Arrigo, K. R., Asanuma, I. *et al.* 2006. A comparison of global estimates of marine primary production from ocean color. *Deep Sea Research Part II: Topical Studies in Oceanography*, 53: 741–770.
- Chassot, E., Bonhommeau, S., Dulvy, N. K., Mélin, F., Watson, R., Gascuel, D., and Le Pape, O. 2010. Global marine primary production constrains fisheries catches. *Ecology Letters*, 13: 495–505.
- Cheung, W. W. L., Lam, V. W. Y., Sarmiento, J. L., Kearney, K., Watson, R., Zeller, D., and Pauly, D. 2010. Large-scale redistribution of maximum fisheries catch potential in the global ocean under climate change. *Global Change Biology*, 16: 24–35.
- Cheung, W. W., Watson, R., Morato, T., Pitcher, T. J., and Pauly, D. 2007. Intrinsic vulnerability in the global fish catch. *Marine Ecology Progress Series*, 333: 1–12.
- Clarke, A., and Fraser, K. P. P. 2004. Why does metabolism scale with temperature? *Functional Ecology*, 18: 243–251.
- Clarke, A., and Johnston, N. M. 1999. Scaling of metabolic rate with body mass and temperature in teleost fish. *Journal of Animal Ecology*, 68: 893–905.
- Conti, L., Grenouillet, G., Lek, S., and Scardi, M. 2012. Long-term changes and recurrent patterns in fisheries landings from large marine ecosystems (1950–2004). *Fisheries Research*, 119: 1–12.
- Dunne, J. P., Armstrong, R. A., Gnanadesikan, A., and Sarmiento, J. L. 2005. Empirical and mechanistic models for the particle export ratio. *Global Biogeochemical Cycles*, 19, GB4026.
- Flood, M., Ilona, S., Andrews, J., Ashby, C., Begg, G., Fletcher, W. J., Gardner, C. *et al.* 2014. Status of Key Australian Fish Stocks Reports 2014. Fisheries Research and Development Corporation.
- Food and Agriculture Organization. 2014. The State of World Fisheries and Aquaculture. Technical Report of the Food and Agriculture Organization of the United Nations. Rome, Italy.
- Free, C. M., Thorson, J. T., Pinsky, M. L., Oken, K. L., Wiedenmann, J., and Jensen, O. P. 2019. Impacts of historical warming on marine fisheries production. *Science*, 363: 979–983.
- Friedland, K. D., Stock, C., Drinkwater, K. F., Link, J. S., Leaf, R. T., Shank, B. V., Rose, J. M. *et al.* 2012. Pathways between primary production and fisheries yields of large marine ecosystems. *PLoS One*, 7: 1932–6203.

- Galbraith, E. D., Carozza, D. A., and Bianchi, D. 2017. A coupled human-earth model perspective on long-term trends in the global marine fishery. *Nature Communications*, 8: 14884.
- Gelchu, A., and Pauly, D. 2007. Growth and Distribution of Port-based Global Fishing Effort within Countries' EEZs from 1970 to 1995. Faculty Research and Publications. Fisheries Centre. University of British Columbia. <https://open.library.ubc.ca/collections/facultyresearchandpublications/52383/items/1.0074748> (last accessed 20 March 2020).
- Gordon, H. S. 1954. The economic theory of a common-property resource: the fishery. *Journal of Political Economy*, 62: 124–142.
- Grainger, R., and Garcia, S. M. 1996. *Chronicles of Marine Fishery Landings (1950-1994): Trend Analysis and Fisheries Potential*. FAO, Rome.
- Guiet, J., Aumont, O., Poggiale, J.-C., and Maury, O. 2016. Effects of lower trophic level biomass and water temperature on fish communities: a modelling study. *Progress in Oceanography*, 146: 22–37.
- Hilborn, R., and Ovando, D. 2014. Reflections on the success of traditional fisheries management. *ICES Journal of Marine Science*, 71: 1040–1046.
- Jennings, S., Mélin, F., Blanchard, J. L., Forster, R. M., Dulvy, N. K., and Wilson, R. W. 2008. Global-scale predictions of community and ecosystem properties from simple ecological theory. *Proceedings of the Royal Society of London B: Biological Sciences*, 275: 1375–1383.
- Locarnini, R. A., Mishonov, A. V., Antonov, J. I., Boyer, T. P., and Garcia, H. E. 2006. *World Ocean Atlas 2005, Volume 1: Temperature*. S. Levitus, Ed. NOAA Atlas NESDIS 61, U.S. Government Printing Office, Washington, DC. 182 pp.
- Lotze, H. K., Tittensor, D. P., Bryndum-Buchholz, A., Eddy, T. D., Cheung, W. W. L., Galbraith, E. D., Barange, M. *et al.* 2019. Global ensemble projections reveal trophic amplification of ocean biomass declines with climate change. *Proceedings of the National Academy of Sciences of the United States of America*, 116: 12907–12912.
- MacCall, A. D. 1990. *Dynamic Geography of Marine Fish Populations*. Washington Sea Grant Program, Seattle, WA.
- Marra, J., Trees, C. C., and O'Reilly, J. E. 2007. Phytoplankton pigment absorption: a strong predictor of primary productivity in the surface ocean. *Deep Sea Research Part I: Oceanographic Research Papers*, 54: 155–163.
- Maureaud, A., Hodapp, D., van Denderen, P. D., Hillebrand, H., Gislason, H., Spaanheden Dencker, T., Beukhof, E. *et al.* 2019. Biodiversity–ecosystem functioning relationships in fish communities: biomass is related to evenness and the environment, not to species richness. *Proceedings of the Royal Society. Biological Sciences*, 286: 20191189.
- Pauly, D., and Zeller, D. 2015. *Sea around Us Concepts, Design and Data*. www.seaaroundus.org.
- Pauly, D., and Zeller, D. 2016. Catch reconstructions reveal that global marine fisheries catches are higher than reported and declining. *Nature Communications*, 7: 10244.
- Rall, B. C., Brose, U., Hartvig, M., Kalinkat, G., Schwarzmüller, F., Vucic-Pestic, O., and Petchey, O. L. 2012. Universal temperature and body-mass scaling of feeding rates. *Philosophical Transactions of the Royal Society of London B: Biological Sciences*, 367: 2923–2934.
- Schaefer, M. B. 1954. Some aspects of the dynamics of populations important to the management of the commercial marine fisheries. *Inter-American Tropical Tuna Commission Bulletin*, 1: 23–56.
- Sherman, K., and Duda, A. M. 1999. Large marine ecosystems: an emerging paradigm for fishery sustainability. *Fisheries*, 24: 15–26.
- Stock, C., and Dunne, J. 2010. Controls on the ratio of mesozooplankton production to primary production in marine ecosystems. *Deep Sea Research Part I: Oceanographic Research Papers*, 57: 95–112.
- Stock, C. A., John, J. G., Rykaczewski, R. R., Asch, R. G., Cheung, W. W. L., Dunne, J. P., Friedland, K. D. *et al.* 2017. Reconciling fisheries catch and ocean productivity. *Proceedings of the National Academy of Sciences*, 114: E1441–E1449.
- Swartz, W., Sala, E., Tracey, S., Watson, R., and Pauly, D. 2010. The spatial expansion and ecological footprint of fisheries (1950 to present). *PLoS One*, 5: e15143.
- United Nations Development Programme. 2016. *Human Development Report 2016: Human Development for Everyone*. <http://hdr.undp.org/en/2016-report> (last accessed 20 March 2020).
- Ursin, E. 1984. The tropical, the temperate and the arctic seas as media for fish production. *Dana*, 3: 43–60.
- Van Denderen, P. D., Lindegren, M., MacKenzie, B. R., Watson, R. A., and Andersen, K. H. 2018. Global patterns in marine predatory fish. *Nature Ecology & Evolution*, 2: 65.
- Watson, R., Zeller, D., and Pauly, D. 2014. Primary productivity demands of global fishing fleets. *Fish and Fisheries*, 15: 231–241.
- Watson, R. A. 2017. A database of global marine commercial, small-scale, illegal and unreported fisheries catch 1950–2014. *Scientific Data*, 4, 170039.
- Watson, R. A., Cheung, W. W., Anticamara, J. A., Sumaila, R. U., Zeller, D., and Pauly, D. 2013. Global marine yield halved as fishing intensity redoubles. *Fish and Fisheries*, 14: 493–503.
- Worm, B., Hilborn, R., Baum, J. K., Branch, T. A., Collie, J. S., Costello, C., Fogarty, M. J. *et al.* 2009. Rebuilding global fisheries. *Science*, 325: 578–585.

Handling editor: Ken Andersen